ACTA MECHANICA SINICA (English Series), Vol.14, No.2, May 1998 ISSN 0567-7718
The Chinese Society of Theoretical and Applied Mechanics
Chinese Journal of Mechanics Press, Beijing, China
Allerton Press, INC., New York, U.S.A.

# HEATING CHARACTERISTICS OF BLUNT SWEPT FIN-INDUCED SHOCK WAVE TURBULENT BOUNDARY LAYER INTERACTION

Tang Guiming (唐贵明)
(*LHD, Institute of Mechanics, Chinese Academy of Sciences, Beijing* 100080, *China*)

**ABSTRACT**: An experimental study was conducted on shock wave turbulent boundary layer interactions caused by a blunt swept fin-plate configuration at Mach numbers of 5.0, 7.8, 9.9 for a Reynolds number range of $(1.0 \sim 4.7) \times 10^7/\mathrm{m}$. Detailed heat transfer and pressure distributions were measured at fin deflection angles of up to 30° for a sweepback angle of 67.6°. Surface oil flow patterns and liquid crystal thermograms as well as schlieren pictures of fin shock shape were taken. The study shows that the flow was separated at deflection of 10° and secondary separation were detected at deflection of $\theta \geq 20°$. The heat transfer and pressure distributions on flat plate showed an extensive plateau region followed by a distinct dip and local peak close to the fin foot. Measurements of the plateau pressure and heat transfer were in good agreement with existing prediction methods, but pressure and heating peak measurements at $M \geq 6$ were significantly lower than predicted by the simple prediction techniques at lower Mach numbers.

**KEY WORDS**: fin, shock wave boundary layer interaction, hypersonic flow, heat transfer

## 1 INTRODUCTION

The large aerothermal loads and severe flow distortions that are generated in three dimensional (3-D) regions of shock wave/turbulent boundary layer interaction are of serious concern to the designers of hypersonic vehicles. The 3-D interaction flows are not easily predicted, even with the most sophisticated computational techniques. The problem is particularly complex for 3-D flow interactions. A majority of studies of 3-D interaction flow have been experimental and most of the data exist on the characteristics of sharp upswept fin interaction in supersonic flows[1]. Hayes[2] and Scuderi[3] have correlated their data and formulated relatively simple expressions for peak pressure and heating rates. However, most of the practical fins are blunt swept fins. The main objective of this study was to examine the aerothermal characteristics of 3-D interaction regions induced by a blunt swept fin in the high Mach number, high Reynolds number flow regime, where little or no data existed, and to determine whether or not the simple predict methods based on the experimental data of sharp unswept fin interactions could be adequate for estimating blunt swept fin

Received 31 October 1997
* The project supported by China Academy of Launch Vehicle Technology

interaction flows. The tests were conducted at free-stream Mach number of 5 to 9.9 and Reynolds number range of $(1.0 \sim 4.7) \times 10^7$/m. Besides detailed measurements of surface heat transfer and pressure on both the flat plate and the windward fin surface, shock schlieren pictures, oil flow patterns and liquid crystal thermograms[4] were taken. Data comparisons were made with existing predict techniques based on the test data at lower Mach numbers.

## 2 EXPERIMENTAL DETAILS

The tests were carried out in the diameter 1.2m test section of the gun tunnel of the Chinese Academy of Sciences with the following test condition, free stream Mach numbers of 5, 7.8, 9.9 and the corresponding freestream unit Reynolds numbers of $4.7 \times 10^7, 3.5 \times 10^7, 1.0 \times 10^7$/m. The Reynolds numbers were high enough to enable turbulent boundary layer to develop upstream of the fin apex.

The test model is shown in Fig.1, which consisted of a blunt fin with a sweep angle of 67.6° and a flat plate 350 mm wide by 550 mm long with a 15° sharp leading edge. The fin had a leading edge radius of 2.5 mm, a semi-wedge angle of 5.08° in the plane normal to the leading edge and the chord length of 153.9 mm. It was mounted to a circular insert on the flat plate at about 350 mm from the plate leading edge. Thus the fin may be set to various deflection angles, $\theta$, of the fin symmetric plane relative to the freestream flow. In this study the deflection angles ranged from $\theta = 0°$ to 30° in 10° increments.

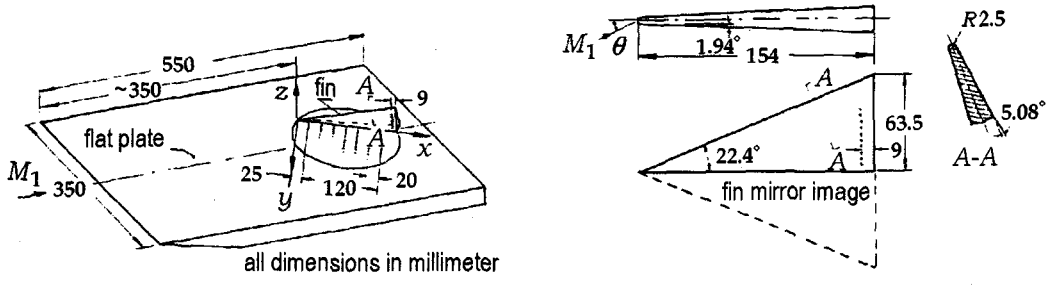


(a) Blunt swept fin mounted on flat plate (b) Blunt swept fin and delta wing

Fig.1 Test models

The circular insert was a part of the flat plate and contained 150 sensors in 7 rows normal to the fin foot chord. Surface heat transfer distributions were measured using platinum thin film gages that were mounted on glass strips such that spatial resolutions of 2mm were obtained in key area of the interaction. Pressure distributions were measured using Kulite transducers. The heating and pressure data were recorded with A/D converter and processed with a 486 microcomputer. Surface flow patterns were obtained by special surface oil dot technique and liquid crystal thermography[4] respectively. Besides these measurements, flowfield schlieren photography was used to determine the inviscid shock wave shape induced by the fin.

## 3 RESULTS AND DISCUSSION

### 3.1 Inviscid Shock Wave Shape

When the fin leading edge is swept back the position of the shock wave without any interaction is unknown and either experiments or calculations must be made to find it. How-

ever, the shock shape or shock angle, $\theta_s$, is only known for sharp unswept fins from oblique shock theory. For the present purposes, it is primarily necessary to know the intersection line of the inviscid shock on the flat plate. $M_1 \sin\theta_s$ is useful as a measure of the strength of the interaction and the correlation parameter of the interaction. In this study the experiment method was chosen to determine the shock shape. A corresponding delta wing (one blunt swept fin and its mirror image) was constructed and was mounted on the test section centerline. Schlieren photographs were taken in elevation and shown in Fig.2(a). From Fig.2(a) we can see that the shock wave attaches at the wing apex for the present test conditions. The pictures gave the shock wave position $\theta_s$ without the wall boundary layer and this shock wave is defined here as the "inviscid shock". A summary of the schlieren results for $\theta_s(M_1, \theta)$ is plotted in Fig.2(b). Clearly, $\theta_s$ is a strong function of $\theta$, but a mild function of $M_1$. The data are prerequisites for the following correlation of fin-induced interaction data.

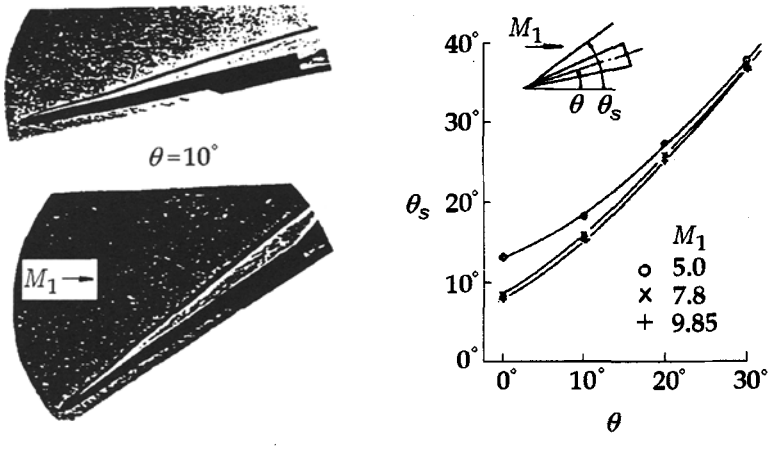


(a) Schlieren photographs ($M_1 = 7.8$) (b) Shock wave angles

Fig.2 Schlieren photographs and shock wave angles on delta wing center-line

### 3.2 The Interaction Flow Features on the Flat Plate

The oil flow pattern, liquid crystal thermogram, distributions of heating and pressure show that at fin deflection of $\theta = 0°$, the fin does not cause upstream interaction and latter separation. Because the fin shock is not strong enough to cause separation at $\theta = 0°$. At $\theta = 10°$, the boundary layer in the interaction region is separated. The oil accumulation and divergence lines can be observed, which correspond to the separation line $S_1$ and attachment line $A_1$ respectively. But compared with the case of fin deflection $\theta = 20°$, no secondary separation was observed. At $\theta \geq 20°$, where the interaction becomes quite strong, secondary separation region is observed on the flat plate. The oil flow pattern and liquid crystal thermogram on the plate at fin deflection of 30° are shown in Fig.3 and Fig.4 respectively. We can observe another pair of convergent line ($S_2$) and divergent line ($A_2$) between $S_1$ and $A_1$. This indicates that there exists a secondary separation ($S_2A_2$) beneath the primary separation ($S_1A_1$) in this case. We also observed the similar flowfields at Mach numbers of 5.0 and 9.9. The comparisons of the results show that the separation lines ($S_1, S_2$) in the oil flow pattern (Fig.3) correspond to the lower temperature lines in liquid crystal thermogram (Fig.4), and the lower heating positions in heating distributions (Fig.5); the attachment

lines $(A_1, A_2)$ correspond to the peak temperature lines and the peak heating positions respectively. The heating and pressure distributions (Fig.5) are characterized by a rise at the separation line $S_1$, then a plateau at attachment line $A_2$ followed a dip at the secondary separation line $S_2$ and a high peak at $A_1$ near the fin foot. The results show that the flow features of the swept fin interaction in hypersonic flows, such as the multiply peaked shape of heating and pressure distributions and the conical nature of the interaction, are qualitatively similar to that of sharp unswept fin in supersonic flows[5].

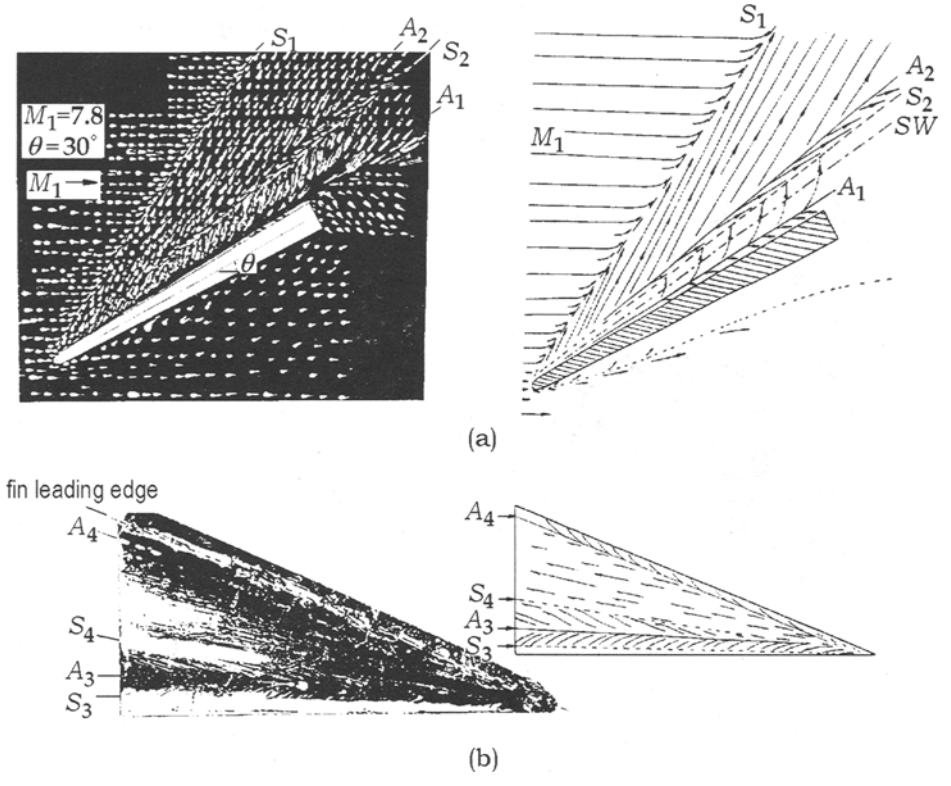


Fig.3 Example of oil flow patterns on flat plate (a) and windward fin surface (b)

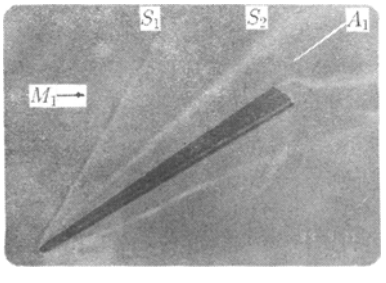


Fig.4 Liquid crystal thermogram on fin interaction region for $M_1 = 7.8, \theta = 30°$

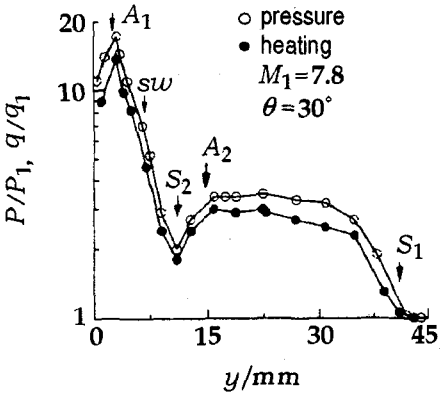


Fig.5 Pressure and heating distributions at $x/\delta = 17$ on flat plate

### 3.3 Peak Pressure and Peak Heat Transfer

Figure 6 shows the variation of normalized peak pressure and heating data with fin deflection $\theta$ and distance, $x/\delta$, parallel to the fin foot chord, where $\delta$ is the turbulent boundary layer thickness at the fin apex and $P_1, q_1$ are the respective undisturbed values of pressure and heating rate on the flat plate. From Fig.6 we can see that peak pressure and peak heating increase with both fin deflection $\theta$ and $x/\delta$. Hayes[2] have correlated the experiment data over a Mach number range from 3 to 5.85 and formulated the following relatively simple expressions for peak pressure and peak heating

$$P_{pk}/P_1 = (M_1 \sin\theta_s)^{n_p} \tag{1}$$

where

$$n_p = \begin{cases} 1.4 + 1.1(x/\delta)/(3.8 + x/\delta) & x < 38\delta \\ 2.4 & x > 38\delta \end{cases}$$

$$q_{pk}/q_1 = n_q(M_1 \sin\theta_s - 1) + 0.75 \tag{2}$$

where

$$n_q = \begin{cases} 1 + \dfrac{2}{3}(x/\delta) & x < 5\delta \\ 4.3 + 0.01(x/\delta) & x > 5\delta \end{cases}$$

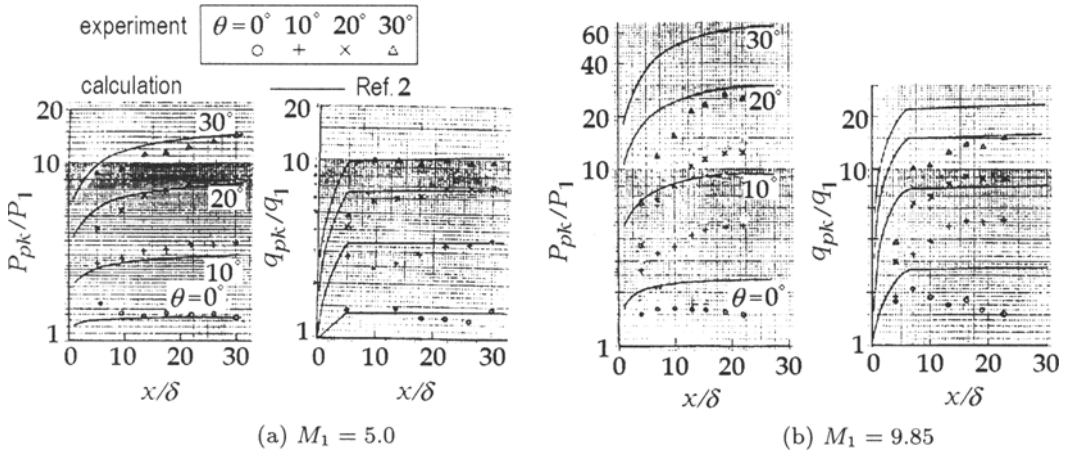


(a) $M_1 = 5.0$ (b) $M_1 = 9.85$

Fig.6 Variation of peak pressure and peak heating with distance from fin apex

The calculated values from Eqs.(1) and (2) are also shown in Fig.6 and are in good agreement with the experiment data at Mach number of 5.0, but are higher than the data at $M_1 = 7.8, 9.9$, and the discrepancy increases with increasing Mach number. Equations (1) and (2) were based on the data at $M_1 < 6$ and may be not adequate for estimating the pressure and heating peak values at $M_1 \geq 6$. Scuderi[3] also observed that the maximum peak pressure increases with shock strength, $M_1 \sin\theta_s$, and obtained an approximation expression

$$P_{mpk}/P_1 = 1.167(M_1 \sin\theta_s)^{2.2} - 0.167 \tag{3}$$

A curve for this expression is included in Fig.7 and is also in good agreement with the data at $M_1 = 5.0$, but is higher than the data at $M_1 = 7.8$ and 9.9. A good approximation to the correlation of the present data is obtained when the exponent in Eq.(3) $n = 4.21/M_1^{0.4}$, namely

$$P_{mpk}/P_1 = 1.167(M_1 \sin\theta_s)^{n} - 0.167 \tag{4}$$

where $n = 4.21/M_1^{0.4} \qquad (M_1 \geq 5)$

The calculated curves from Eq.(4) are also shown in Fig.7.

The peak heating, $q_{pk}/q_1$, can be also related to the peak pressure, $P_{pk}/P_1$, by a simple power law relation, namely,

$$q_{pk}/q_1 = (P_{pk}/P_1)^k \qquad k = 0.9 \tag{5}$$

The comparison of calculation and the present data is shown in Fig.8.

We find that the rays on which peak heating and pressure are located overlap each other. The peak locations are in good agreement with the values predicted by Token's expression[6],

$$\phi_{pk} = 0.24(\theta_s - \theta_F) + \theta_F \tag{6}$$

where $\theta_F = \theta + 1.94°$.

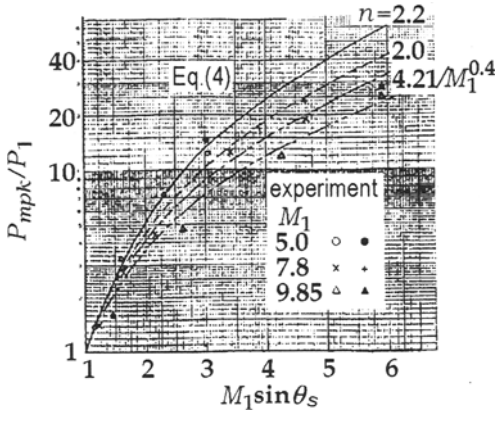


Fig.7 Comparison of maximal peak pressure measurements with calculation

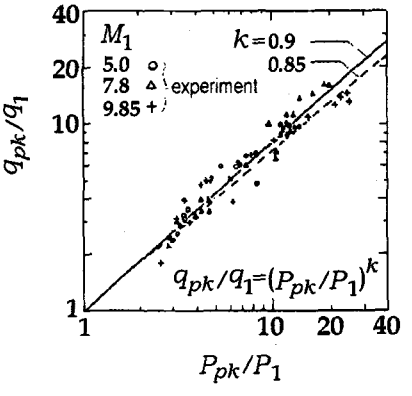


Fig.8 Correlation of peak heating vs peak pressure

### 3.4 Plateau Pressure and Plateau Heat Transfer

Scuderi[3] and Hayers[2] observed that the plateau pressure data, $P_{\text{plat}}/P_1$, in the interaction region induced by a unswept sharp fin correlate well with $(M_1 \sin\theta_s)$. Zukuski[7] also observed that the plateau pressure in the 2D interaction region induced by a forward facing step can correlate well with shock strength. Their expressions for predicting plateau pressure are as follow,

$$P_{\text{plat}}/P_1 = 2.75(M_1 \sin\theta_s)^{0.5} - 1.75 \tag{7}$$

$$P_{\text{plat}}/P_1 = 0.41 + 0.91(M_1 \sin\theta_s) - 0.06(M_1 \sin\theta_s)^2 \tag{8}$$

$$P_{\text{plat}}/P_1 = 1 + \frac{1}{2} M_1 \sin\theta_s \tag{9}$$

Equations (7) and (8) were derived by Scuderi[3] and Hayes[2] based on their experiment data with Mach number ranging from 3.0 to 5.85 respectively. The comparison of the present data with calculations is shown in Fig.9. Our measurements of plateau pressure are in good agreement with the calculations based on the Eqs.(8) and (9), but the calculated values from Scuderi's expression (7) is higher than that from Eqs.(8) and (9), and our test data when $M_1 \sin\theta_s > 2.5$. The plateau pressure is a result of the boundary layer separation and its magnitude is independent of the method used to generate the separation. Therefore data

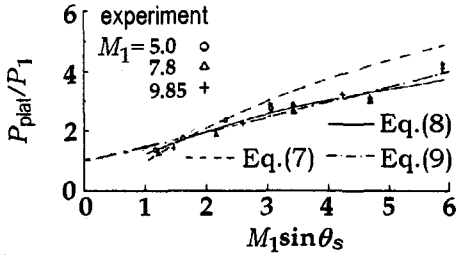


Fig.9 Comparison of plateau pressure measurements with predictive methods

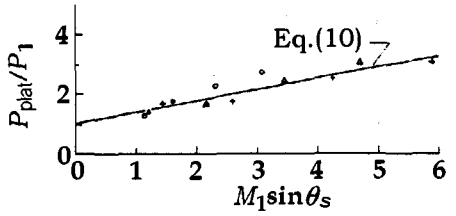


Fig.10 Plateau heating correlation

from 2D interaction such as a step and 3D interaction such as a sharp fin correlate well in the plateau region.

Correlation of plateau heating data with plateau pressures is presented in Fig.10. The expression approximating the present data of plateau heating is

$$q_{\text{plat}}/q_1 = (P_{\text{plat}}/P_1)^{0.85} = \left(1 + \frac{1}{2}M_1 \sin\theta_s\right)^{0.85} \tag{10}$$

Our measurements of plateau heat transfer are in reasonable agreement with Eq.(10).

### 3.5 Pressure and Heating Distributions on the Windward Surface of the Fin

We find that when fin deflection is big enough, for example, $\theta \geq 20°$, two pairs of separation lines $S_3, S_4$ and attachment lines $A_3, A_4$ exist also on the oil flow pattern on the fin surface, as shown in Fig.4. High pressure and heating peak and dip also occur at the corresponding positions on the fin surface. Figure 11 shows pressure and heating distributions along a span ray on the fin surface at a deflection of 30° for Mach number of 7.8, and the feature positions of the separation line $S_3, S_4$ and attachment line $A_3$ obtained from the oil flow pattern shown in Fig.4. The results show that when $\theta \geq 20°$, flow separation also occurs on the fin surface. Little data exist on the fin side surface, peak pressure and heating correlations is not available up to date.

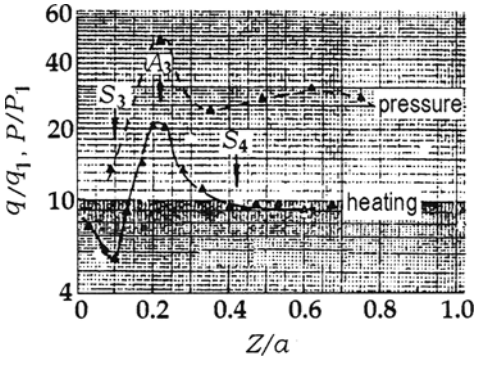


Fig.11 Typical pressure and heating distributions on windward fin surface for $M_1 = 7.8, \theta = 30°$

## 4 CONCLUSION

No disturbance exists ahead of 67.6° swept fin apex at $M_1 \geq 5$ and deflection up to 30°, because shock wave induced by the blut fin attaches at its apex foot.

When the fin deflection is big enough, the turbulent boundary layer is separated on flat plate as well as on windward fin surface. The conical nature of the hypersonic interaction flow induced by the blunt swept fin is qualitatively similar to that of supersonic interaction induced by a sharp upswept fin.

When secondary separation occurs, two pairs of separation and attachment line exist on the flat plate, and occur on the fin windward side as well, resulting in multiple peaked pressure and heating distributions. The positions of peak heat transfer and peak pressure correspond to the peak temperature lines in the liquid crystal thermogram and the attachment lines on the oil flow pattern.

Plateau pressure, plateau heating, peak pressure and peak heating can correlate well with shock strength $M_1 \sin\theta_s$. Our measurements of plateau pressure are in good agreement with the calculations based on both the 3D correlations of Hayes and the 2D correlations of Zukoski.

Peak pressure and peak heat transfer predicted by the correlations of Hayes are in good agreement with the data at Mach number of 5.0, but is higher than the data at Mach numbers of 7.8 and 9.9.

## REFERENCES

1 Stollery JL. Glancing shock-boundary layer interactions. AGARD No.764
2 Hayes JR. Prediction techniques for the characteristics of fin generated three dimensional shock wave turbulent boundary layer interactions. AD A042024, 1977
3 Scuderi LF. Expressions for predicting 3-D shock wave-turbulent boundary layer interaction pressures and heating rates. AIAA Paper, 1978. 78~162
4 Tang GM. Surface oil flow technique and liquid crystal thermography for flow visualization in impulse wind tunnels. *Acta Mechanica Sinica*, 1994, 10(3): 220~226
5 Settles GF, Lu FK. Conical similarity of shock/boundary layer interaction generated by swept and unswept fins. *AIAA J*, 1985, 23(7): 1021~1027
6 Token KH. Heat transfer due to shock wave turbulent boundary layer interactions on high speed weapon systems. AFFDL-TR-74-77, 1974
7 Zukoski EE. Turbulent boundary-layer separation in front of a forward-facing step. *AIAA J*, 1967, 5(10): 1746~1753